Okamoto *et al. J Wood Sci* (2021) 67:8
https://doi.org/10.1186/s10086-021-01941-3

Journal of Wood Science

ORIGINAL ARTICLE

Open Access

Study on the strength of glued laminated timber beams with round holes: difference in structural performance between homogeneous-grade and heterogeneous-grade timber

Shigefumi Okamoto[1*], Nobuhiko Akiyama[2], Yasuhiro Araki[2], Kenji Aoki[3] and Masahiro Inayama[3]

Abstract

Various design codes and design proposals have been proposed for glued laminated timber beams with round holes, assuming that the entire beam is composed of homogeneous-grade timber. However, in Japan, glued laminated timber composed of homogeneous-grade timber is rarely used for beams. In this study, the difference in the load-bearing capacity of glued laminated beams composed of homogeneous-grade timber and heterogeneous-grade timber with round holes when fractured by cracking was investigated experimentally and analytically. The materials used in the tests were glued laminated beams composed of homogeneous-grade Scots pine timber with a strength grade of E105-F345 and heterogeneous-grade Scots pine timber with a strength grade of E105-F300. Experiments confirmed that although the glued laminated beams composed of heterogeneous-grade timber have a lower material strength in the lamina with holes, its resistance to fracturing due to cracks associated with the holes is almost the same as that of the glued laminated beams composed of homogeneous-grade timber. The stresses acting on the holes in the laminated timber with holes of less than half the beam height were lower in the glued laminated beams composed of heterogeneous-grade timber than in the glued laminated beams composed of homogeneous-grade timber. The ratio of the stresses was found to be approximately equal to the ratio of the maximum bending stress or the maximum shear stress acting on the inner layer lamina, as determined by Bernoulli–Euler theory.

Introduction

When the shear force and bending moment act on a glued laminated timber beam with a round hole, the beam will undergo flexural fracture if the ratio of the bending moment is high. However, if the rate of shear forces acting on the beam is high, it will fracture through the development of cracks associated with the holes [1]. In real buildings, holes are often located near the support points of beams. Therefore, holes are located where high shear forces and small bending moments occur.

As shown in Fig. 1, a large tensile stress perpendicular to the grain acts on the crack plane of the hole in the beam affected by the shear force or bending moment, and the tensile stress decreases exponentially with distance from the hole [2]. Various design codes and design proposals for glued laminated timber beams with round holes have been presented [1–6]. The design code in the Swedish Glulam handbook [4] and DIN EN 1995-1-1/NA [5] is a method for estimating the fracture strength by calculating the tensile stress perpendicular to the grain acting on the 45° portion shown in Fig. 1. The design proposal of Aicher [2], [2] incorporates the size effect

*Correspondence: okamoto@osaka-cu.ac.jp
[1] Graduate School of Human Life Science, Osaka City University, 3-3-138 Sugimoto, Sumiyoshi-ku, Osaka 558-8585, Japan
Full list of author information is available at the end of the article

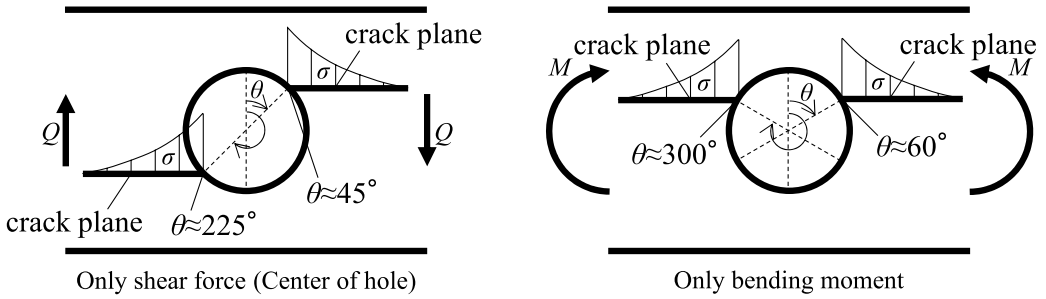

Fig. 1 Distribution of tensile stress perpendicular to the grain in the highest stress zone around the hole

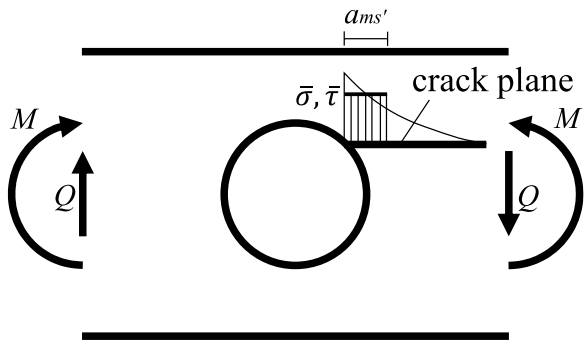

Fig. 2 Mean stress method

Fig. 2 Mean stress method

of Weibull's statistical theory into the methods of the design code [4, 5]. The design proposal of Noguchi [3] is a method for estimating the fracture strength using the fracture energy of fracture mode 1. The design proposal of Hijikata [1] is a method for estimating the fracture strength by calculating the maximum principal stress acting around holes. These design codes and design proposals calculate the stresses acting on the holes, assuming that the beams are entirely composed of homogeneous wood.

In Japan, glued laminated beams composed of heterogeneous-grade timber, as specified in Japanese Agricultural Standard (JAS) [7], are very often used as beams, and it is not known whether the presented design codes and design proposals [1–6] can be used. Therefore, in [8], it was confirmed that the stresses acting on a hole in a glued laminated beam composed of heterogeneous-grade timber can be accurately estimated by finite element analysis (FEA) to estimate the load-bearing capacity associated with fracturing due to cracking. In [8], a design equation was proposed to compensate for the average length of the mean stress method [9] (Fig. 2), a generalization of linear elastic fracture mechanics, to take into account the size effect of the portions of the design with large tensile stresses (Eqs. 1, 2). Equations (1, 2) can be used to estimate the bearing capacity related to small and large holes during crack-related fracturing. The analysis in [8] shows that the stress acting on the hole is smaller in the case of a glued laminated beam composed of heterogeneous-grade timber than in the case of a glued laminated beam composed of homogeneous-grade timber:

$$\sqrt{(\bar{\sigma}/F_{t90})^2 + (\bar{\tau}/F_s)^2}/k_{\mathrm{vol}} \leqq 1.0, \tag{1}$$

$$k_{\mathrm{vol}} = \left(\frac{30}{\max(0.2D, 30)}\right)^{0.14},$$

$$a'_{\mathrm{ms}} = \frac{a_{\mathrm{ms}}}{1 + \frac{a_{\mathrm{ms}}}{\alpha \cdot D}}, \tag{2}$$

$$a_{\mathrm{ms}} = \frac{2}{\pi}\frac{E_{\mathrm{I}} \cdot G_{\mathrm{Ic}}}{F_{t90}^2},$$

$$E_{\mathrm{I}} = \sqrt{\frac{2 \cdot E_x \cdot E_y}{\sqrt{\frac{E_x}{E_y}} + \frac{E_x}{2 \cdot G_{xy}} - \nu_{xy}}},$$

where D is the diameter of the hole, F_{t90} is the tensile strength perpendicular to the grain, F_s is the shear strength, $\bar{\sigma}$ and $\bar{\tau}$ are the mean values of the tensile stress σ and the shear stress τ perpendicular to the grain in the potential fracture area of length a_{ms}' (Fig. 2), k_{vol} is the factor of size effect, G_{Ic} is the mode I fracture energy, E_x is Young's modulus parallel to the grain, E_y is Young's modulus perpendicular to the grain, G_{xy} is the shear modulus, ν_{xy} is Poisson's ratio, α is a constant (1 for $D/H \leq 1/3$), and H is the beam height. Since $\bar{\sigma}$ is the dominant stress at failure, a_{ms} is set to the value of pure mode I.

Therefore, in this study, the difference in load-bearing capacity when fracturing occurs by cracks in beams with round holes was investigated using glued laminated beams composed of heterogeneous-grade timber and homogeneous-grade timber with the same Young's modulus of bending as specified in JAS [7]. First, bending tests were performed on the beams to experimentally investigate the difference in load-bearing capacity when fractured due to cracks. We then estimated the experimental values using Eqs. (1, 2) to analytically investigate the differences in structural performance. Finally, the stresses acting on the holes in glued laminated beams composed of heterogeneous-grade timber and glued laminated beams composed of homogeneous-grade timber were determined by FEA and compared. We then examined the reduction rate of stress acting on the holes in the case of glued laminated beams composed of heterogeneous-grade timber, which is specified in JAS [7].

The results of the bending tests of beams, material experiments and experimental specification FEA for glued laminated beams composed of heterogeneous-grade timber are the same as those reported in [8]. In this paper, a new study conducted on glued laminated timber beams composed of homogeneous-grade to determine the difference in structural performance between homogeneous-grade and heterogeneous-grade glued laminated timber beams with round holes in comparison with the results reported previously is presented.

Materials and methods

Bending tests of beams

The materials used are glued laminated beams composed of heterogeneous-grade timber and homogeneous-grade timber as specified by JAS [7] for Scots pine. The strength grade of the glued laminated beams composed of heterogeneous-grade timber is E105-F300, and the strength grade of the glued laminated beams composed of homogeneous-grade timber is E105-F345. A schematic diagram and the specifications of the test specimens are shown in Fig. 3. The lamina arrangement of the glued laminated timber used for the test specimens is shown in Fig. 4. The beam width B of the test specimens is 105 mm, and the beam heights H are 150 mm, 300 mm and 450 mm. The hole diameters D are $H/3$, $H/5$,

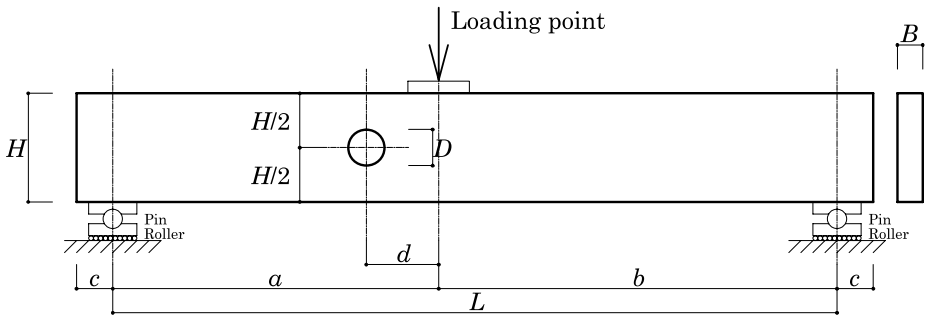

Tree species	B (mm)	H (mm)	L (mm)	a (mm)	b (mm)	c (mm)	d (mm)	D (mm)	Strength grade	Compose	Number of specimens
Scots pine	105	150	1000 ($H\times20/3$)	450 ($H\times9/3$)	550 ($H\times11/3$)	150	100 ($H\times2/3$)	30 ($H/5$)	E105-F345	Homogeneous-grade	2
									E105-F300	Heterogeneous-grade	3
								50 ($H/3$)	E105-F345	Homogeneous-grade	2
									E105-F300	Heterogeneous-grade	3
		300	2000 ($H\times20/3$)	900 ($H\times9/3$)	1100 ($H\times11/3$)	150	200 ($H\times2/3$)	30 ($H/10$)	E105-F345	Homogeneous-grade	2
									E105-F300	Heterogeneous-grade	3
								60 ($H/5$)	E105-F345	Homogeneous-grade	2
									E105-F300	Heterogeneous-grade	3
								100 ($H/3$)	E105-F345	Homogeneous-grade	2
									E105-F300	Heterogeneous-grade	3
		450	3000 ($H\times20/3$)	1350 ($H\times9/3$)	1650 ($H\times11/3$)	150	300 ($H\times2/3$)	30 ($H/15$)	E105-F345	Homogeneous-grade	2
									E105-F300	Heterogeneous-grade	3
								90 ($H/5$)	E105-F345	Homogeneous-grade	2
									E105-F300	Heterogeneous-grade	3
								150 ($H/3$)	E105-F345	Homogeneous-grade	2
									E105-F300	Heterogeneous-grade	3

Fig. 3 Test specimens and specifications

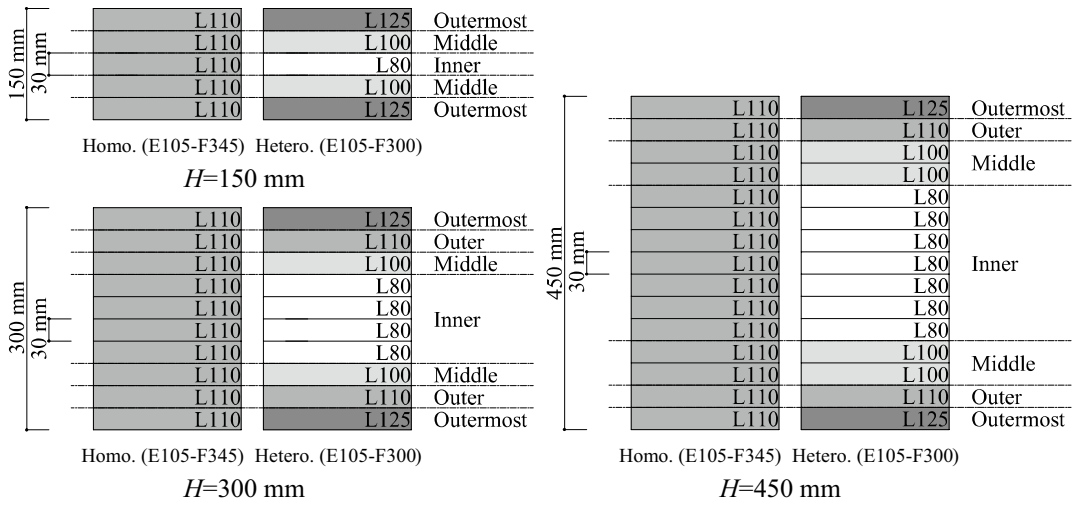

Fig. 4 Lamina arrangement of the glued laminated timber used in the experiment

$H/10$ ($H=300$ mm only) and $H/15$ ($H=450$ mm only). In [8], we conducted bending tests on glued laminated timber composed of heterogeneous-grade with D/H of 2/3 and 4/5, but since it is considered difficult to incorporate glued laminated timber with large hole diameters into the design code, these D/H values were excluded from this study. The number of test specimens is two for each type of glued laminated beam composed of homogeneous-grade timber and three for each type of glued laminated beam composed of heterogeneous-grade timber. The mean and standard deviation values of density were 531 ± 6 kg/m^3 for the glued laminated beams composed of homogeneous-grade timber and 522 ± 11 kg/m^3 for the glued laminated beams composed of heterogeneous-grade timber. Density is the weight of the test object divided by the volume. The mean and standard deviation values of moisture content were $12.7 \pm 4.2\%$ for the glued laminated beams composed of homogeneous-grade timber and $13.1 \pm 3.2\%$ for the glued laminated beams composed of heterogeneous-grade timber. The moisture content was measured by a moisture meter (HM-530, Kett Electric Laboratory). The experiment was carried out at a crosshead speed of 6 mm/min to ensure that the load was applied for more than 1 min from the start of loading to fracturing. Displacement gauges were placed at the load and support points to obtain the deflection of the load points.

Material tests

Tests were conducted to determine the shear strength, tensile strength perpendicular to the grain, and mode I fracture energy at the crack locations associated with the holes in the glued laminated timber beams. The materials used were L80-grade and L110-grade Scots pine in the inner layer position shown in Fig. 4.

The shear strength parallel to the grain was determined by the test method with a standard shear block specimen (Fig. 5a) according to JIS Z 2101 [10]. Twenty L80-grade specimens for and ten L110-grade specimens were cut from the beams used in the bending tests (Fig. 5b). The size of the shear surface was 30 mm × 30 mm. The experiment was conducted at a constant crosshead speed, and the load was applied so that the time between the start of the load loading and fracturing was approximately 1 min. The mean and standard deviation values of density were 463 ± 12 kg/m^3 for L80-grade and 530 ± 18 kg/m^3 for L110-grade. The moisture content of the specimen was not measured because the moisture content of the beams was measured.

It has been reported that the flexural strength of concrete decreases with increasing specimen height and approaches the tensile strength [11]. In [8], timber specimen heights of 20 mm, 40 mm, 150 mm, and 300 mm were tested in flexural tests, and it was shown that the flexural strengths of timber specimens with heights of 150 mm and 300 mm were nearly the same. Based on these facts, in [8], the bending strength obtained in bending tests with a specimen height of 150 mm was taken as the tensile strength perpendicular to the grain of the timber. Although not a standard test method, in this study, the bending strength obtained by the bending test method shown in Fig. 6 was also used as the tensile strength perpendicular to the grain of the timber. Bending test methods are also specified in ISO 13910 [12], although they yield a fairly low tensile strength at the lower boundary limit. The

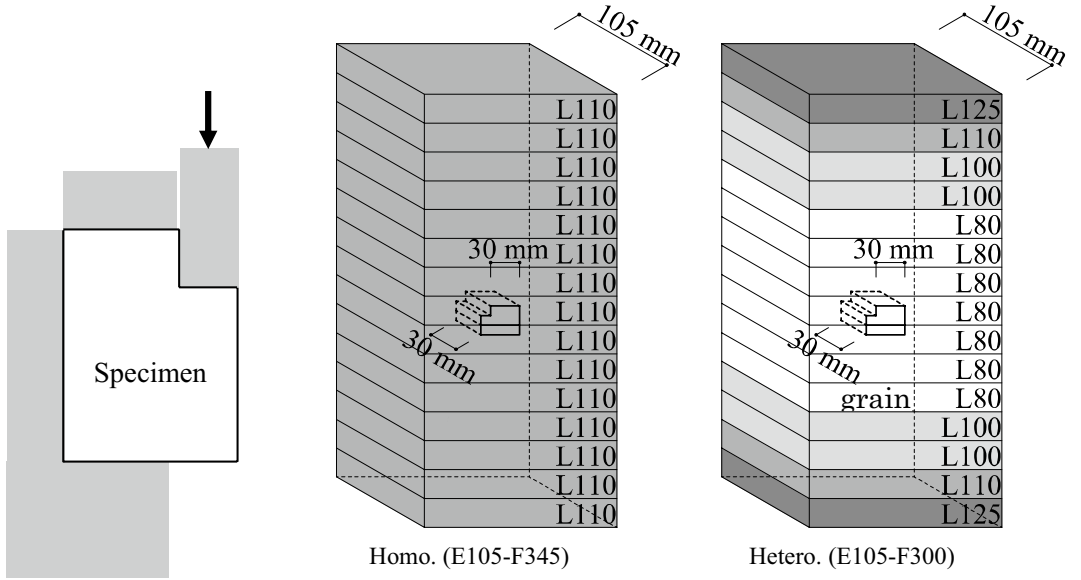

Fig. 5 Schematic diagram of the shear test

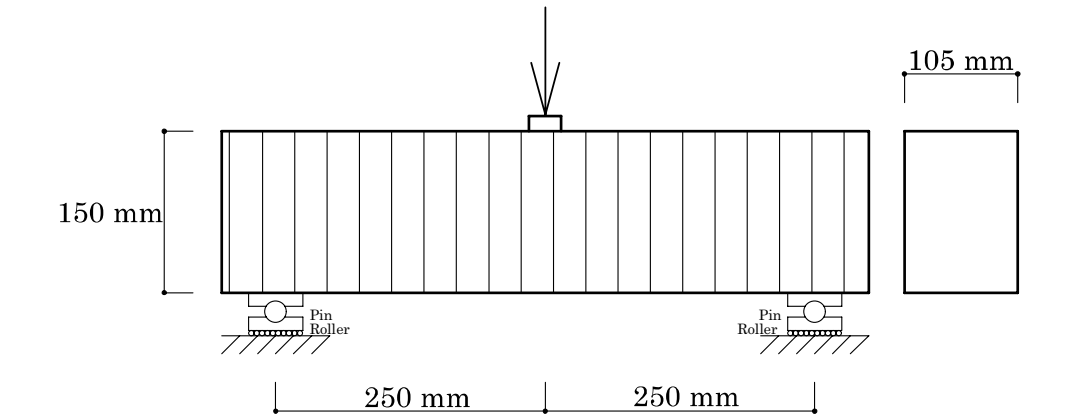

Fig. 6 Schematic diagram of the tension test perpendicular to the grain

tensile strength perpendicular to the grain was determined using the same bending test method as in [8], as shown in Fig. 6. The test specimens were glued laminated beams composed of L80-grade and L110-grade timber. The number of specimens was six each. The experiment was conducted at a constant crosshead speed and applied load, and the speed was adjusted so that 1 to 2 min elapsed from the start of load loading to fracturing. The mean and standard deviation values of density were 485 ± 6 kg/m^3 for the L80-grade timber and 510 ± 2 kg/m^3 for the L110-grade timber. The mean and standard deviation values of moisture content were 10.7 ± 2.0% for the L80-grade timber and 8.0 ± 0.7% for the L110-grade timber.

The test method for obtaining the fracture energy G_{Ic} of fracture mode I fractures is the single-edge-notched bending test [13] shown in Fig. 7. The height of the specimens was in accordance with the specifications in [13], and the width of the specimens was 105 mm, the same as the specimens in the bending tests. The test specimens were glued laminated beams composed of L80-grade timber and glued laminated beams composed of L110-grade timber. The number of specimens was set to 10 each. The experiment was conducted at a constant crosshead

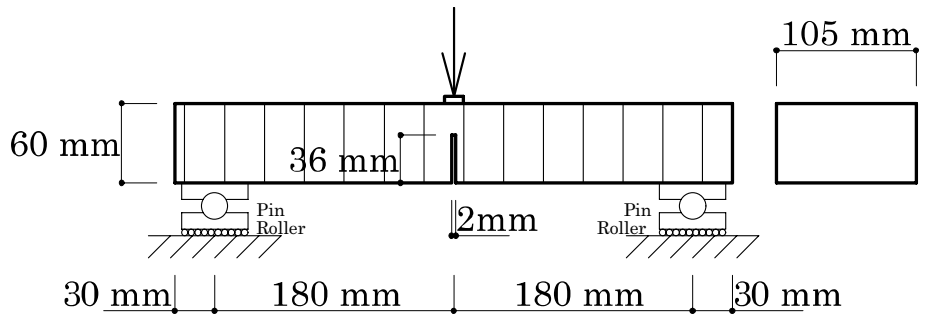

Fig. 7 Schematic diagram of the single-edge-notched bending test

speed, and the load was applied so that the time between the start of the load loading and fracture was approximately 3 min. The mean and standard deviation values of density were 475 ± 6 kg/m^3 for the L80-grade timber and 532 ± 8 kg/m^3 for the L80-grade timber. The mean and standard deviation values of moisture content were 8.6 ± 1.8% for the L80-grade timber and 8.7 ± 1.1% for the L80-grade timber.

Finite element analysis

The stresses acting on the holes in the beam were determined by two-dimensional finite element analysis (2D-FEA). ANSYS 18.2 was used for 2D-FEA. The specifications applied in the 2D-FEA were those of the bending tests and cases in which only the shear force or bending moment acts on the center of the hole. The details of the 2D-FEA are described below:

1. Specifications of the bending tests

   The numerical finite element (FE) model was set up such that the stress acting on the hole was the same as that in the bending tests, as shown in Fig. 8. The numerical FE model is representative of the same glued laminated beam composed of heterogeneous-grade timber as in [8] and the glued laminated beam composed of homogeneous-grade timber with modified laminate material properties. The specimen specifications in the bending tests in which the holes were fractured by cracks were analyzed. The

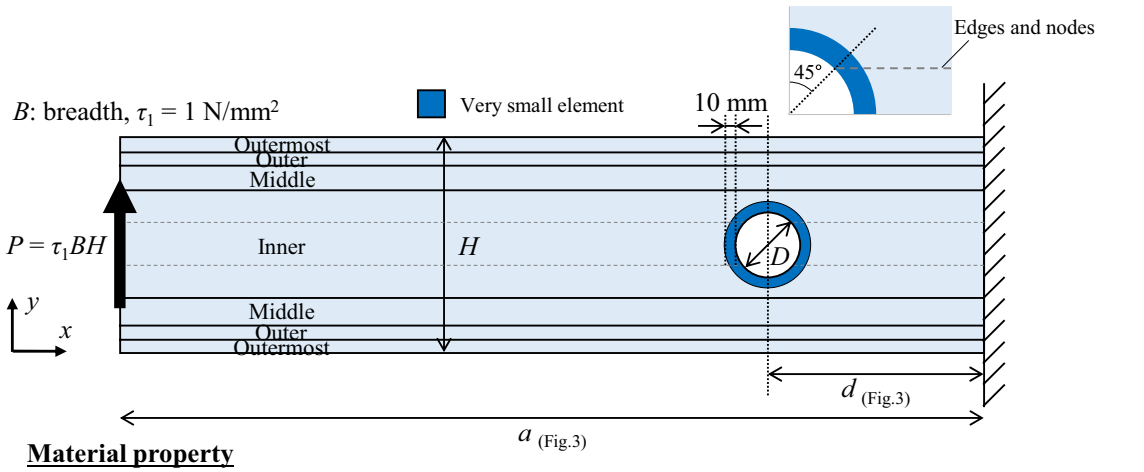

Material property

$E_y = E_x / 25$, $G_{xy} = E_x / 15$, $\nu_{xy} = 0.4$

E_x: Homogeneous-grade (E105-F345)

Outermost: 11100 N/mm^2, Outer: 11000 N/mm^2, Middle: 11000 N/mm^2, Inner: 11000 N/mm^2

Heterogeneous-grade (E105-F300)

Outermost: 12500 N/mm^2, Outer: 11000 N/mm^2, Middle: 10000 N/mm^2, Inner: 8000 N/mm^2

Fig. 8 Geometry and material properties of the FE model

material parameters of the elements were determined in the same way as in [8]. The Young's modulus parallel to the grain was set to the Young's modulus of the bending of lamina as shown in JAS [7] (E_x = 11,000 N/mm^2 for L110). The Young's modulus perpendicular to the grain was set to $E_y = E_x/25$, the shear modulus was set to $G = E_x/15$, and the Poisson's ratio was set to $\nu_{xy} = 0.4$. The lamina arrangement of the glued laminated timber is shown in Fig. 4. The wood was treated as a four-node planar element, and the elements were less than 10 mm per side (H = 450 mm, H = 300 mm) or less than 5 mm per side (H = 150 mm). The range of 10 mm from the hole was divided into small sections so that the nodes are placed at one degree. To determine the stress distribution at the location of fracturing by the crack, the edges and nodes of the elements were placed in the X direction (direction parallel to the grain) from the $\theta = 45°$ position. The mesh size of the FE model is shown in Fig. 9. We wanted to divide the elements very finely around only the hole, so some 3-node planar elements are placed. Compared with the numerical FE results when all the elements were reduced in size and the number of elements was doubled, the error in the stress around the holes was less than 1%, so we concluded that the optimal solution could be obtained by the element division shown in Fig. 9.

2. Specifications where only shear force or bending moment acts on the center of the hole
   The numerical FE model was set up for the case where the stress at the center of the hole was shear force only ($Q = \tau_1 BH$ (N), $M = 0$, $\tau_1 = 1$ N/mm^2) and bending moment only ($Q = 0$, $M = \tau_1 BH^2$ (Nmm), $\tau_1 = 1$ N/mm^2), as shown in Fig. 10. The values of the shear force and bending moment were set so that the stresses acting on them would be the same at different beam heights H. The D/H values were set to 0.05, 0.1, 0.2, 0.3, 0.4, and 0.5, and the beam height H was set to 300 mm. The material parameters of the elements were the same as in (1). The lamina arrange-

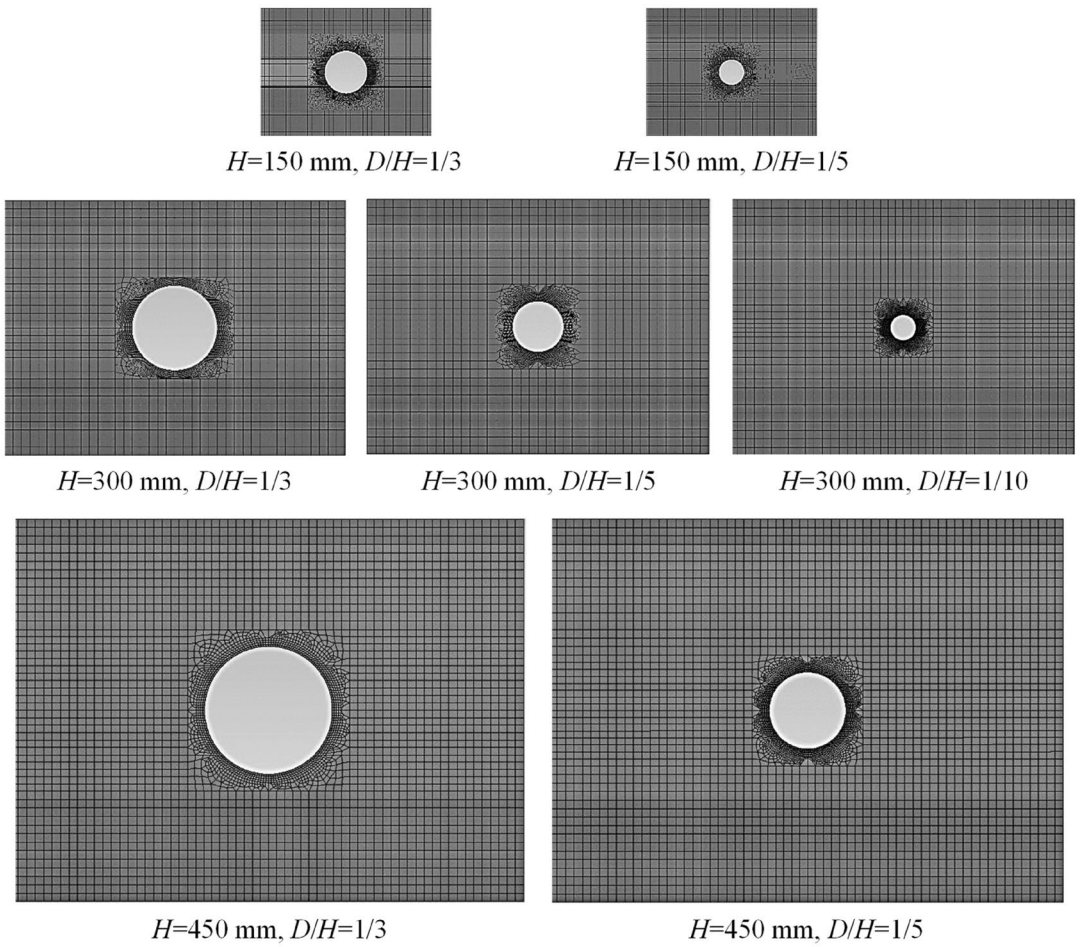

Fig. 9 Mesh size of the FE model from Fig. 8

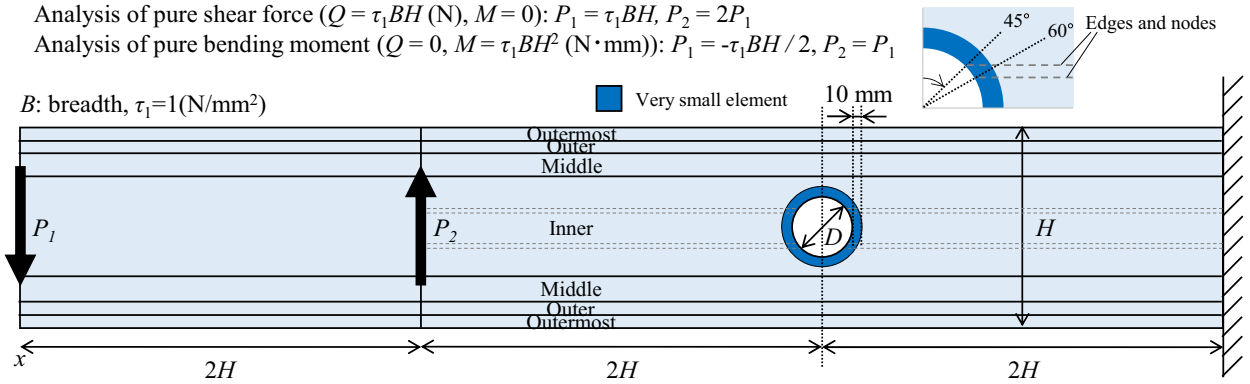

Material property

$E_y = E_x / 25$, $G_{xy} = E_x / 15$, $v_{xy} = 0.4$

E_x: Homogeneous-grade (E105-F345)

Outermost: 11000 N/mm², Outer: 11000 N/mm², Middle: 11000 N/mm², Inner: 11000 N/mm²

Heterogeneous-grade (E105-F300)

Outermost: 12500 N/mm², Outer: 11000 N/mm², Middle: 10000 N/mm², Inner: 8000 N/mm²

Fig. 10 Geometry and material properties of the FE model for pure shear or pure moment loading situations

ment of the glued laminated timber is shown in Fig. 11 according to JAS [7]. The strength grade specified in JAS [7] for the glued laminated beam composed of homogeneous-grade timber was E105-F345. However, the stresses acting on the beams constructed of homogeneous-grade timber are the same for different strength grades. The strength grades specified in JAS [7] for the glued laminated beams composed of heterogeneous-grade timber were E105-F300 and E55-F200. The wood was treated as a four-node planar element, and the elements were less than 5 mm per side. The range of 10 mm from the hole was divided into small sections so that the nodes are placed at one degree. To obtain the stress distribution at the location of the high stress, the edges and nodes of the elements were placed in the X direction (parallel to the grain direction) from the $\theta = 45°$ and 60° positions. The mesh size of the FE model is shown in Fig. 12. Compared with the numerical FE results when all the elements were reduced in size and the number of elements was doubled, the error in the stress around the holes was less than 1%, so

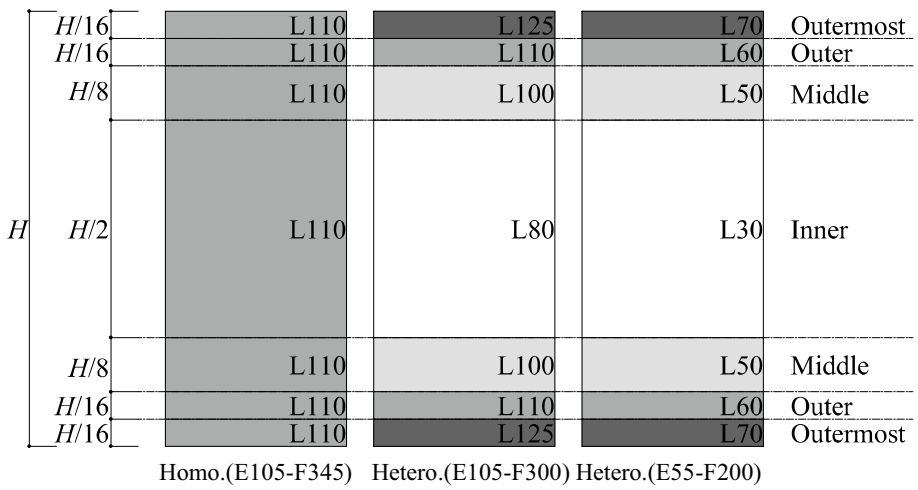

Fig. 11 Lamina arrangement in the glued laminated timber [7]

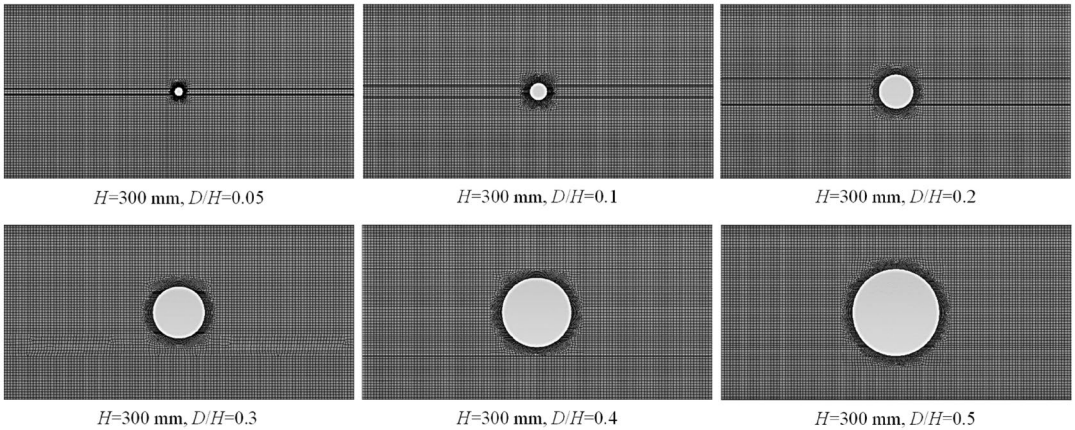

Fig. 12 Mesh size of the FE model from Fig. 10

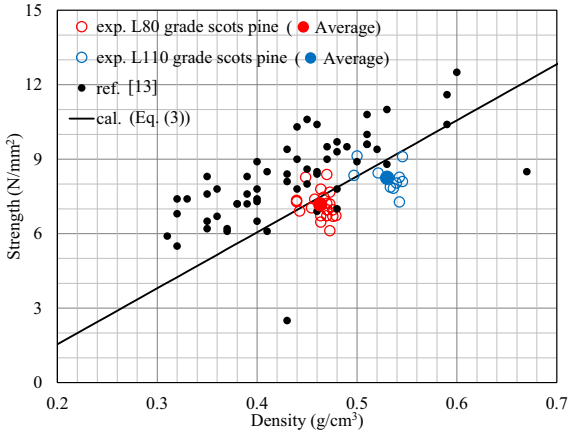

Fig. 13 Shear strength

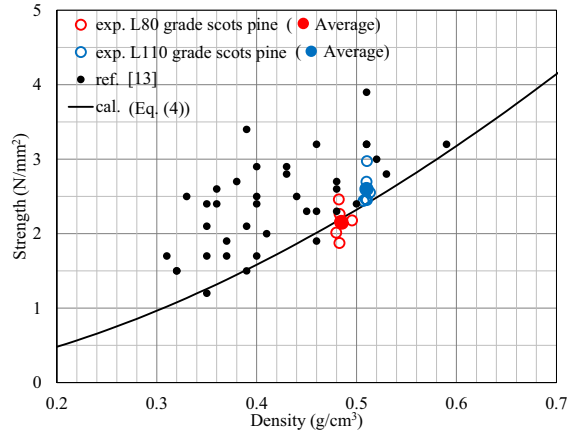

Fig. 14 Tensile strength perpendicular to the grain

we concluded that the optimal solution could be obtained by the element division shown in Fig. 12.

Results and discussion

Material tests

Data on the shear strength parallel to the grain obtained from the material experiments, existing data on the shear strength parallel to the grain for coniferous trees [14], and the relationship between density ρ and shear strength parallel to the grain with a shear surface of 30 mm × 30 mm for 20 tree species (Eq. 3) [15] are shown in Fig. 13. Data on the tensile strength perpendicular to the grain obtained from material experiments, existing data on the tensile strength perpendicular to the grain for coniferous trees [14], and the relationship between density ρ and tensile strength perpendicular to the grain with a tensile cross section of 25 mm × 50 mm for three tree species (Eq. 4) [15] are shown in Fig. 14. The mode I fracture energy obtained from material experiments and the relationship between density ρ and mode I fracture energy for Scots pine (Eq. 5) [16] are shown in Fig. 15. From these comparisons, it was confirmed that the values obtained in the material experiments corresponded approximately to the lower limit of the existing strength data and were in general agreement with the relationships described by Eqs. (3–5). The maximum, minimum, mean and standard deviation of the values obtained in the material experiments are shown in Table 1.

$$F_s\left(\mathrm{N/mm^2}\right) = 22.56 \times \rho - 2.97, \tag{3}$$

$$F_{t90}\left(\mathrm{N/mm^2}\right) = 7.65 \times \rho^{1.72}, \tag{4}$$

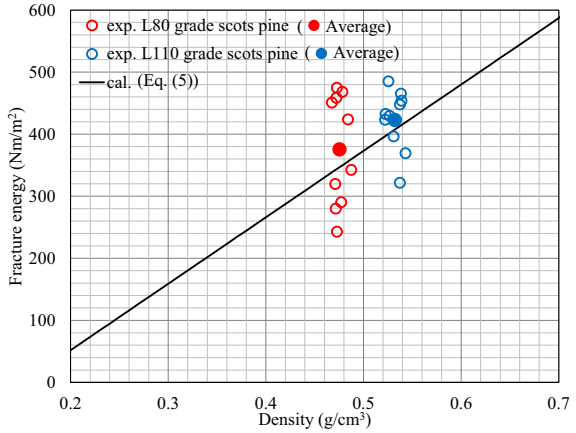

Fig. 15 Fracture energy for mode I

$$G_{Ic}\left(\mathrm{N\cdot m/m^2}\right) = 1070 \times \rho - 162, \tag{5}$$

where ρ (g/cm^3) is the density.

Bending tests of beams

All specimens with $D/H = 1/15$ and one of the glued laminated beams composed of heterogeneous-grade timber with $D/H = 1/10$ fractured during bending without hole-related cracking. Other specimens fractured due to cracks in the holes, as shown in Fig. 16. The specimens with cracks in the hole first exhibited a short crack in the upper part of the force side, and then after the crack had extended to some length, a crack developed in the lower part of the fulcrum side, and the crack extended to the end surface, reducing the bearing capacity. Some specimens also fractured with the formation of all cracks occurring at the same time.

The load–displacement relationship is shown in Fig. 17. The load is the value measured at the force point, and the displacement is the amount of deflection at the force point. In 80% of the specimens where initial cracks could be visually identified, the initial cracks occurred when the deflection at the force point was offset by 0.2 to 0.5 mm. In particular, 0.2 mm was the most common at 36%. The offset values did not change much for different specimen sizes. In [8], the initial crack load was defined

Table 1 Element test results

		Strength grade	Max	Min	Ave	SD
Shear strength parallel to the grain	F_s (N/mm^2)	L110	9.13	7.28	8.24	0.57
		L80	8.38	6.12	7.17	0.57
Tension strength perpendicular to the grain	F_{t90} (N/mm^2)	L110	2.97	2.44	2.60	0.21
		L80	2.46	1.88	2.15	0.20
Fracture energy for Mode I	G_{Ic} (N m/m^2)	L110	485	322	422	49
		L80	475	243	375	89

Tree species: Scots pine

Fig. 16 Final fracture state of holes

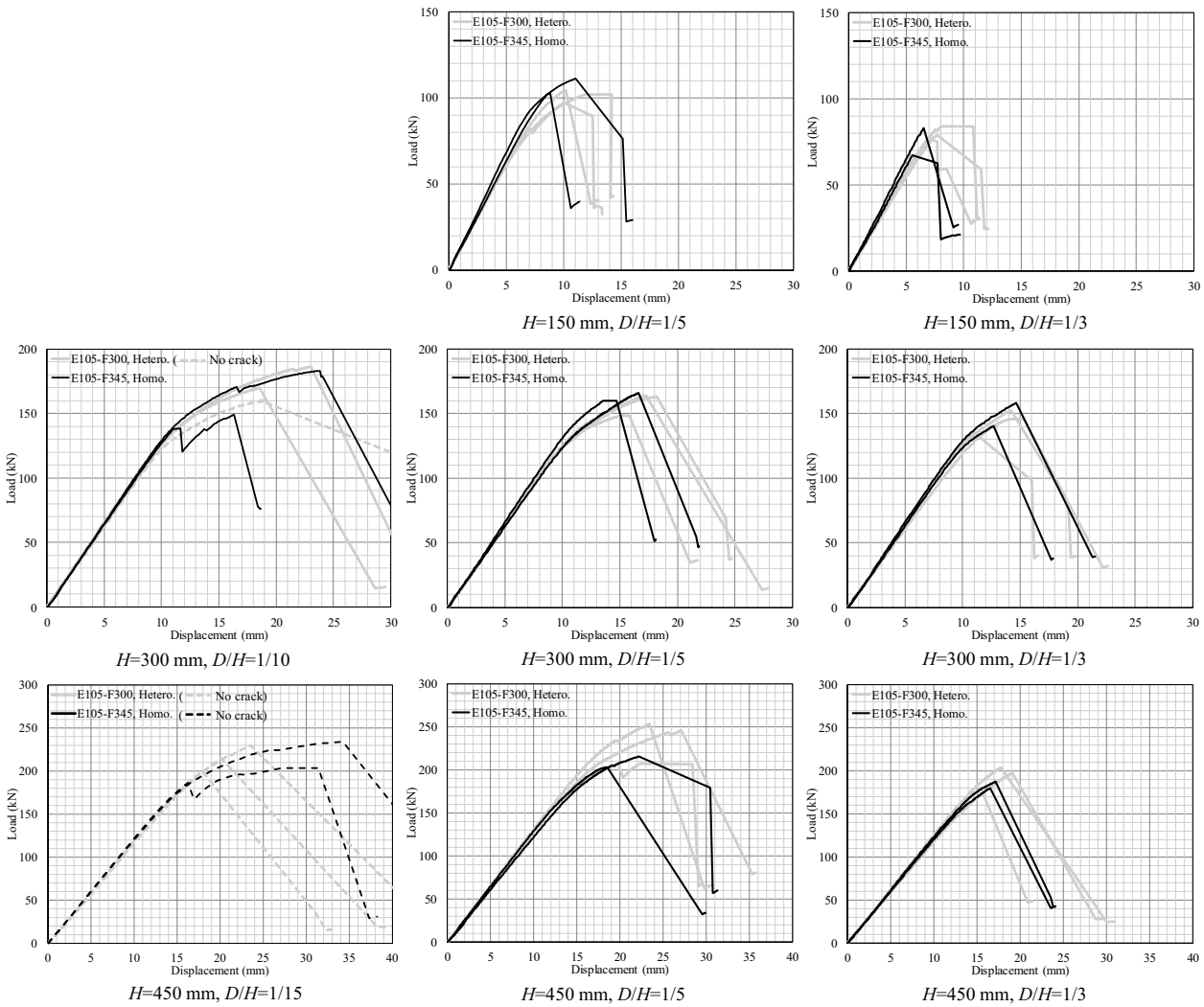

Fig. 17 Load–displacement relationships at the loading point

as the load when the deflection at the force point was offset by 0.2 mm for this reason. In this study, the load at a deflection at the force point of 0.2 mm was defined as the initial crack load in the same way. The maximum loads for all specimens and the initial cracking loads for specimens that failed due to cracking are shown in Table 2. Figure 18 shows the relationship between the ratio of the maximum load or initial crack load to D/H for the glued laminated beams composed of homogeneous-grade and heterogeneous-grade timber. The ratio of the material strength of the inner lamina is also shown as a straight line. Except for the initial cracking load of $D/H=1/5$ at $H=150$ mm, the ratio of the bending tests was smaller than the material properties, and the maximum load and the initial cracking load were not much different between the glued laminated beams made up of homogeneous-grade and heterogeneous-grade timber.

Estimation of experimental values

To analytically investigate the differences in structural performance between the glued laminated beams composed of heterogeneous-grade timber and homogeneous-grade timber, the experimental values were estimated by Eqs. (1, 2). The tensile stress perpendicular to the grain acting around the hole is shown in Fig. 19, which was obtained from the analysis in Fig. 8. The results of the analysis show that when the shear force acting on the hole is $Q=BH\tau_1$ and the hole diameter ratio D/H is constant, the distribution of σ is almost the same. The maximum values of σ are all at $\theta=45°$, and it is assumed that cracks form and extend parallel to the grain direction (X direction) from this position. This is generally consistent with the location of the first crack in the bending tests of beams. The maximum values of σ in Fig. 19 were approximately 14% lower for the glued

Table 2 Maximum load and initial crack load

H (mm)	*D* (mm)	E105-F345, homogeneous-grade						E105-F300, heterogeneous-grade							
		Maximum load (kN)			Initial crack load (kN)			Maximum load (kN)				Initial crack load (kN)			
		No. 1	No. 2	Ave	No. 1	No. 2	Ave	No. 1	No. 2	No. 3	Ave	No. 1	No. 2	No. 3	Ave
150	30 (*H* × 1/5)	111.3	102.9	107.1	90.7	95.1	92.9	97.2	104.5	102.1	101.3	73.3	72.2	66.8	70.8
	50 (*H* × 1/3)	67.4	83.0	75.2	67.4	83.0	75.2	84.0	79.1	76.7	80.0	73.1	68.4	72.9	71.4
300	30 (*H* × 1/10)	149.3	183.2	166.3	133.1	131.6	132.4	186.3	*160.0*	169.8	172.0	123.7	*117.2*	125.6	122.2
	60 (*H* × 1/5)	165.9	160.1	163.0	123.6	133.6	128.6	148.9	164.0	163.0	158.6	122.1	125.0	115.0	120.7
	100 (*H* × 1/3)	140.6	158.4	149.5	121.8	119.1	120.4	135.2	145.8	152.6	144.6	122.1	115.1	121.1	119.4
450	30 (*H* × 1/15)	*203.6*	*234.0*	218.8	*159.5*	*156.8*	158.1	*199.8*	*229.6*	*214.5*	214.6	*154.6*	*152.8*	*163.7*	157.0
	90 (*H* × 1/5)	203.4	215.6	209.5	151.3	137.7	144.5	245.6	253.2	207.5	235.4	160.6	180.7	156.1	165.8
	150 (*H* × 1/3)	187.3	179.7	183.5	147.1	148.1	147.6	197.3	179.9	203.6	193.6	138.9	167.0	159.4	155.1

Initial crack load is the 0.2 mm offset load, italic data—no crack

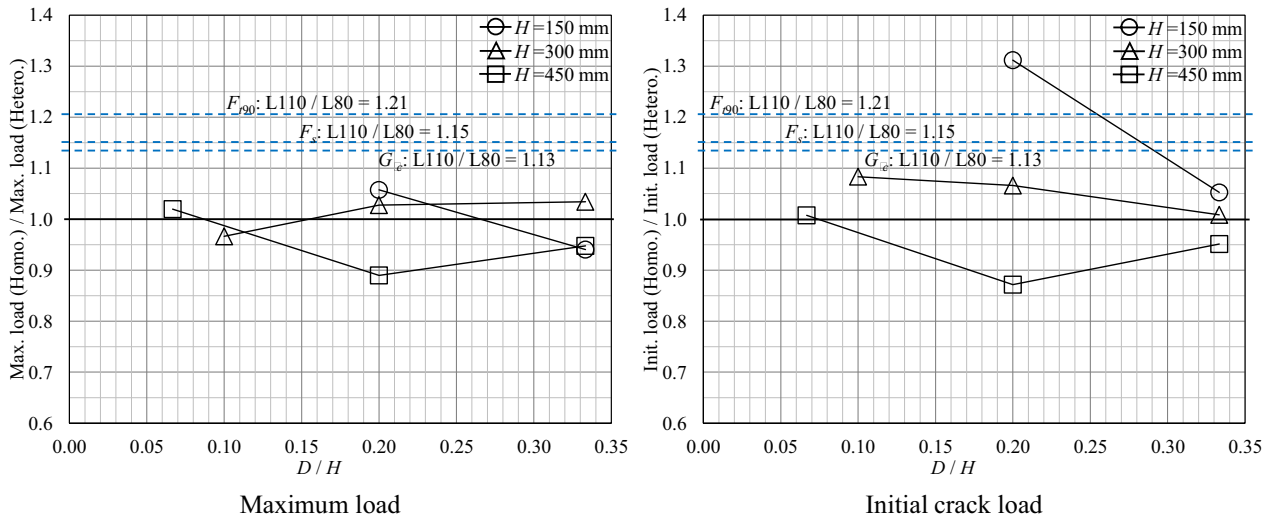

Fig. 18 Ratio of maximum load and initial crack load in the homogeneous-grade timber and heterogeneous-grade timber

laminated beams composed of heterogeneous-grade timber than for the glued laminated beams composed of homogeneous-grade timber at $D/H = 1/3$, 13% lower at $D/H = 1/5$, and 10% lower at $D/H = 1/10$.

The distribution of tensile stresses perpendicular to the grain and shear stresses at the assumed fracture location are shown in Fig. 20. The position around the hole is set to $x = 0$, and the horizontal axis is x/D. The results of the analysis show that the stress distribution is almost the same at different beam heights. The ratio of the stresses in the glued laminated beams composed of homogeneous-grade timber and heterogeneous-grade timber did not change much with the position of x/D, and the ratio was somewhat constant. The average stress for use in Eq. (1) can be found in Eq. (6) using the coefficients in each term in Fig. 20:

$$\overline{\sigma}, \overline{\tau} = \frac{a_6}{7} \cdot \left(\frac{a'_{\mathrm{ms}}}{D}\right)^6 + \frac{a_5}{6} \cdot \left(\frac{a'_{\mathrm{ms}}}{D}\right)^5 + \frac{a_4}{5} \cdot \left(\frac{a'_{\mathrm{ms}}}{D}\right)^4 + \frac{a_3}{4} \cdot \left(\frac{a'_{\mathrm{ms}}}{D}\right)^3 + \frac{a_2}{3} \cdot \left(\frac{a'_{\mathrm{ms}}}{D}\right)^2 + \frac{a_1}{2} \cdot \left(\frac{a'_{\mathrm{ms}}}{D}\right) + a_0. \quad (6)$$

Figure 21 shows a comparison of the calculated and experimental cracking loads in the bending tests calculated by Eqs. (1, 2) using the average values in Table 1. The calculated values for the glued laminated beams composed of homogeneous-grade timber (cal. Eq. (1), Homo. Eq. (2), L110) and for the glued laminated beams composed of heterogeneous-grade timber (cal. Eq. (1),

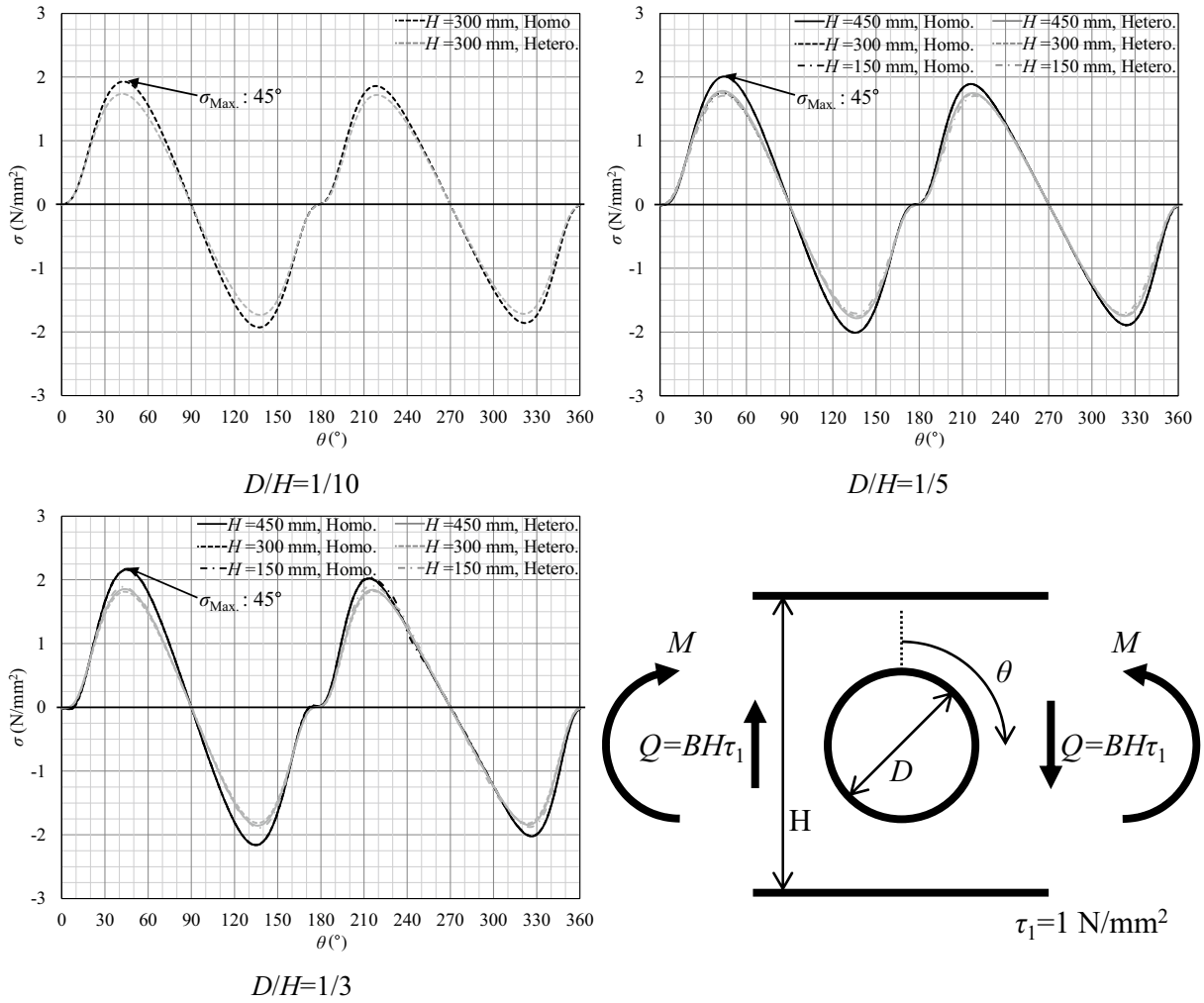

Fig. 19 Tensile stress perpendicular to the grain around the hole

Hetero. Eq. (2), L80) are given. In addition, the calculated values for the stresses in the glued laminated beams composed of homogeneous-grade timber using the material strength of the L80 grade are also given as reference values (cal. Eq. (1), Homo. Eq. (2), L80). The calculated values of $D/H=1/3$ and $D/H=1/5$ are good estimates of the bearing capacity at the initial cracking, and the calculated value of $D/H=1/10$ is approximately halfway between the initial and maximum bearing capacities. The ratio of (calculated value of Homo. L110)/(calculated value of Homo. L80) is 1.21, which is the same as (F_{t90} for L110)/(F_{t90} for L80). However, the ratio (calculated value of Homo. L110)/(calculated value of Hetero. L80) is smaller than the ratio of material properties, as shown in Fig. 18, which is 1.05 for $D/H=1/3$, 1.08 for $D/H=1/5$ and 1.09 for $D/H=1/10$.

For $H=150$ mm, the $D/H=1/3$ specimen of glued laminated beams composed of heterogeneous-grade timber had an initial crack in the lamina of L100-grade timber. Therefore, the calculation results using the material strength of L80-grade timber differed from the actual situation. Young's modulus and density have a linear relationship [17]. The shear strength and mode I fracture energy have a linear relationship with density, as shown in Eqs. (3, 5). Additionally, tensile strength has a nonlinear relationship with density (Eq. 4), but Fig. 14 shows that it can be estimated with a linear relationship. Therefore, because no material testing was performed on the L100-grade timber, it was assumed that its Young's modulus and material strength exhibited a linear relationship, and the material strength of L100-grade timber was estimated from the average material strength of L80-grade and L110-grade timber. The estimated material strength of L100-grade timber was $F_s=7.89$ N/mm^2, $F_{t90}=2.45$ N/mm^2, and $G_{Ic}=407$ Nm/m^2. Figure 21 shows the calculated values for the glued laminated

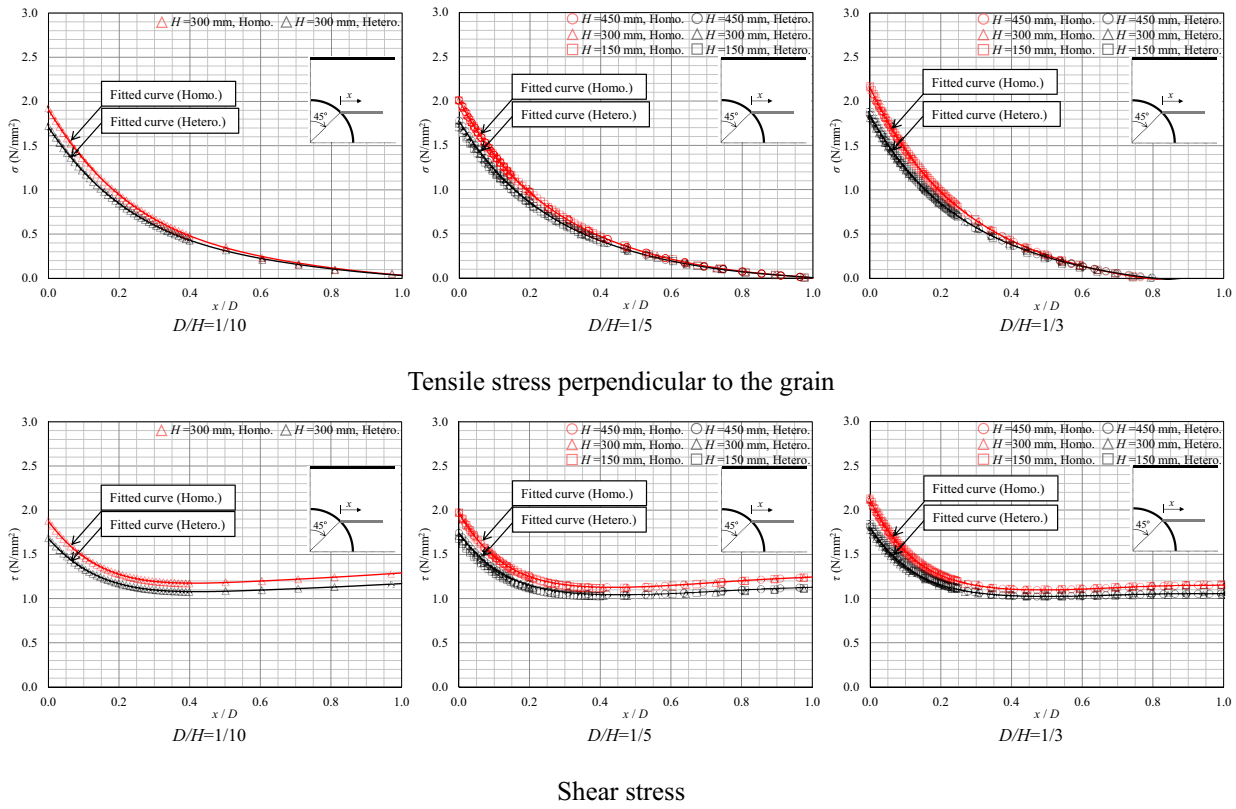

Fig. 20 Stress at the split fracture location

material with $D/H = 1/3$ based on the estimated material strength of L100-grade timber. The ratio (calculated value of Homo. L110)/(calculated value of Hetero. L100) ratio for $D/H = 1/3$ was 0.93.

Differences in stress levels around the hole

Many design codes and design proposals [1–6] also require the tensile stress perpendicular to the grain acting on the holes, assuming that the beams are entirely composed of homogeneous wood. Therefore, the stresses acting on the holes in glued laminated beams composed of heterogeneous-grade timber and glued laminated beams composed of homogeneous-grade timber were determined by the analysis in Fig. 10 and compared. We then examined the reduction rate of stress acting on the holes in the case of the glued laminated beams composed of heterogeneous-grade timber, which is specified in JAS [7].

The tensile stresses perpendicular to the grain and the shear stresses acting on the holes in the glued laminated beams composed of homogeneous-grade timber determined by the numerical FE analysis are shown in Fig. 22. The stresses acting on the hole are symmetric or inversely symmetric with respect to the center of the hole. The tensile stresses perpendicular to the grain and the shear stresses acting on the holes in the glued laminated beams composed of homogeneous-grade timber and glued laminated beams composed of heterogeneous-grade timber (E105-F300 and E55-F200), as determined by the numerical FE analysis, are shown in Figs. 23 and 24. The stresses are shown for only one-quarter of the holes. The ratio of stresses acting on the holes of glued laminated beams composed of the homogeneous-grade and heterogeneous-grade timber was constant with little change in position.

The bending and shear stress distributions from Bernoulli–Euler theory for glued laminated beams composed of heterogeneous-grade timber and glued laminated beams composed of homogeneous-grade timber are shown in Fig. 25a. The ratios of the maximum bending stress (σ_{Inner} in Fig. 25a) to the maximum

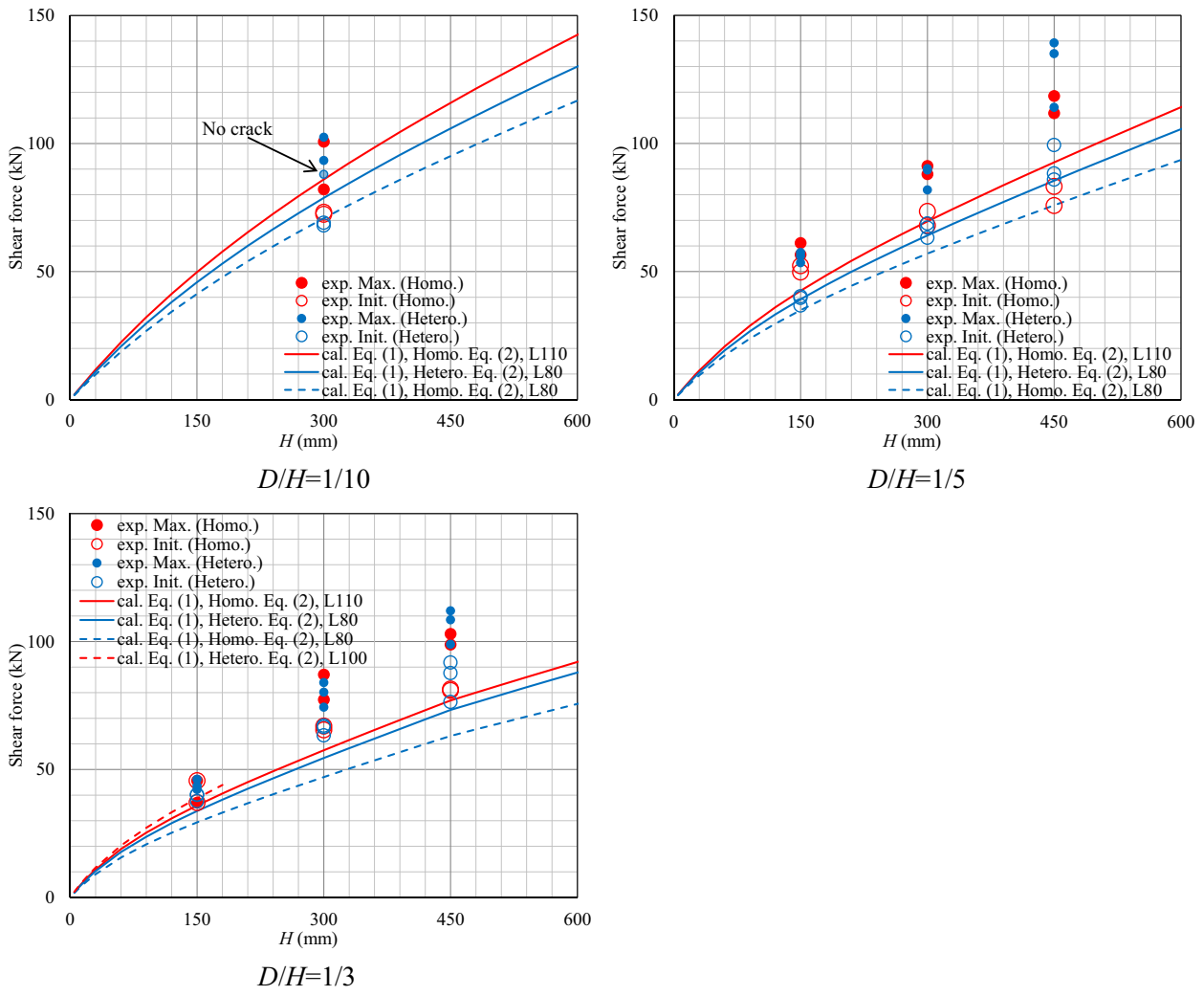

Fig. 21 Experimental and calculated values

shear stress ($\tau_{\mathrm{Max.}}$ in Fig. 25a) in the inner lamina for the same bending moment or the same shear force in the glued laminated beams composed of heterogeneous-grade timber (Fig. 25b) and glued laminated beams composed of homogeneous-grade timber as defined by JAS [7] are shown in Fig. 25c. The ratio of bending stress is k_M and the ratio of shear stress is k_Q. Figure 26 compares the ratio of the maximum stress in Figs. 23 and 24 with k_M and k_Q (Fig. 25c). For small D/H values, the ratios for k_Q and the pure shear force (center of the hole) case obtained by FEA are almost equal, and the ratios for the pure bending moment case obtained by k_M and FEA are almost equal. However, as the D/H increases, the FEA results become smaller than those of k_Q and k_M.

Figures 27 and 28 show the stresses of glued laminated beams composed of homogeneous-grade timber in Figs. 23 and 24 multiplied by k_Q or k_M. Figures 29 and 30 show the distribution of stresses in the direction parallel to the grain (tensile stresses perpendicular to the grain σ and shear stresses τ) at $\theta=60°$ ($y/D=0.25$) and $\theta=45°$ ($y/D=0.35$). The stresses in the glued laminated beams composed of homogeneous-grade timber are multiplied by k_Q or k_M. In the case of small D/H values, the results are almost equal to the stresses in the glued laminated beams composed of heterogeneous-grade timber.

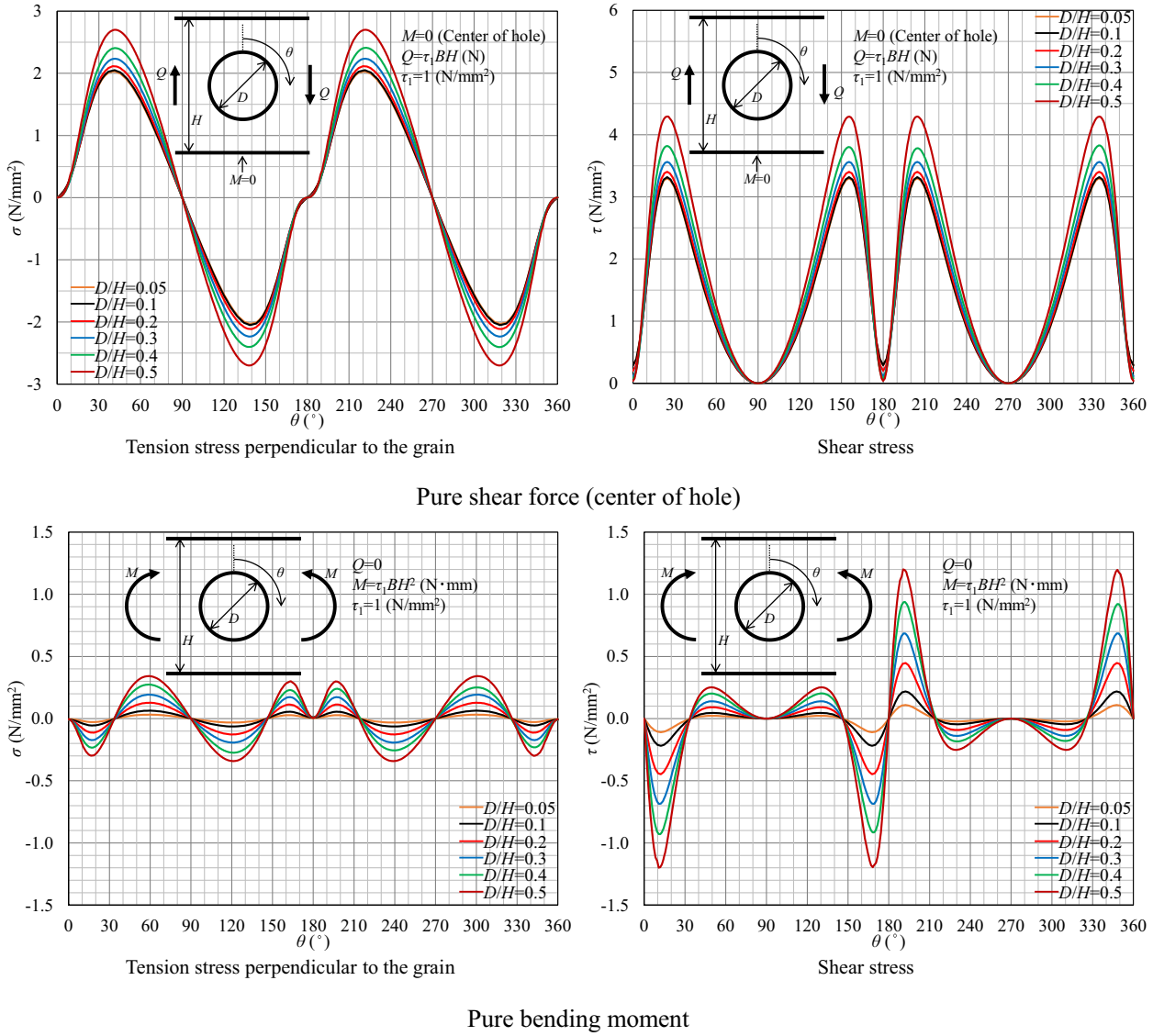

Fig. 22 Stress around the hole, Homo

However, as the D/H increases, the stresses in the glued laminated beams composed of homogeneous-grade timber multiplied by k_Q or k_M tend to be higher.

It can be concluded that when the D/H is low, the stresses in the glued laminated beams composed of homogeneous-grade timber can be multiplied by k_Q or k_M in Fig. 25c to obtain the stresses in the glued laminated beams composed of heterogeneous-grade timber. In addition, if the D/H is less than 0.5, the stresses in the glued laminated beams composed of heterogeneous-grade timber will not be underestimated even when the D/H is large.

Conclusion

In this study, the difference in the load-bearing capacity of glued laminated beams composed of homogeneous-grade timber and heterogeneous-grade timber with round holes when fractured by cracking was investigated experimentally and analytically. The following results were obtained:

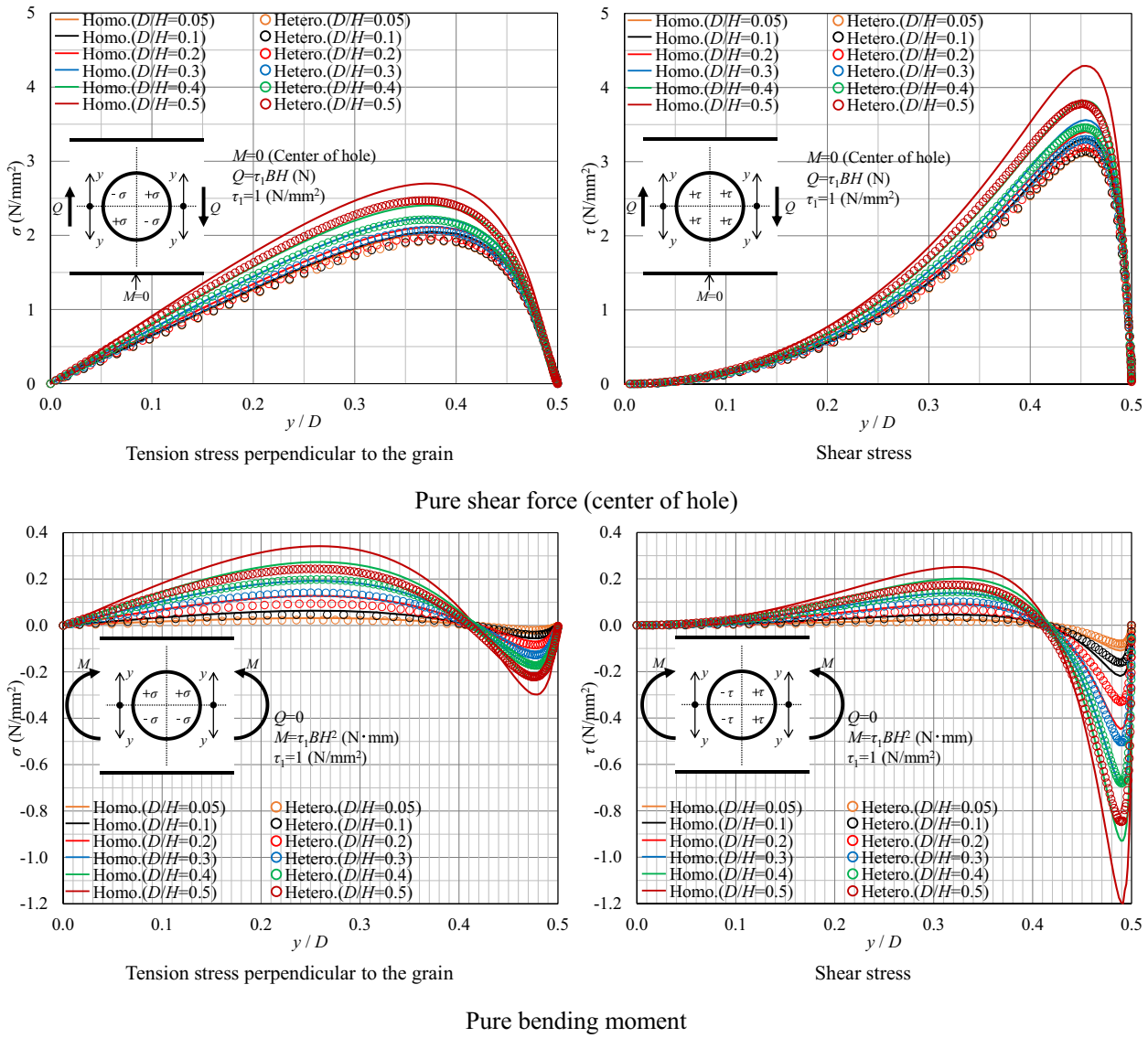

Fig. 23 Stress around the hole, Hetero. E105-F300 and Homo

1. The ratio of material strength (shear strength, tensile stress perpendicular to the grain, and mode I fracture energy) of the inner lamina of glued laminated beams composed of homogeneous-grade timber (E105-F345) and heterogeneous-grade timber (E105-F300) with the same Young's modulus of bending as specified by JAS [7] was 1.13–1.21 in terms of (strength of inner layer lamina (L110) of homogeneous-grade timber)/(strength of inner layer lamina (L80) of heterogeneous-grade timber). However, the (load-bearing capacity of homogeneous-grade timber)/(load-bearing capacity of heterogeneous-grade timber) ratio of resistance to fracturing due to cracking in the bending tests for glued laminated timber beams with round holes ranged from 0.87 to 1.08.
2. The load-bearing capacity of the beams obtained in the bending tests was calculated using FEA and material strength, and it was found that the ratio of (load-bearing capacity of homogeneous-grade timber)/(load-bearing capacity of heterogeneous-grade

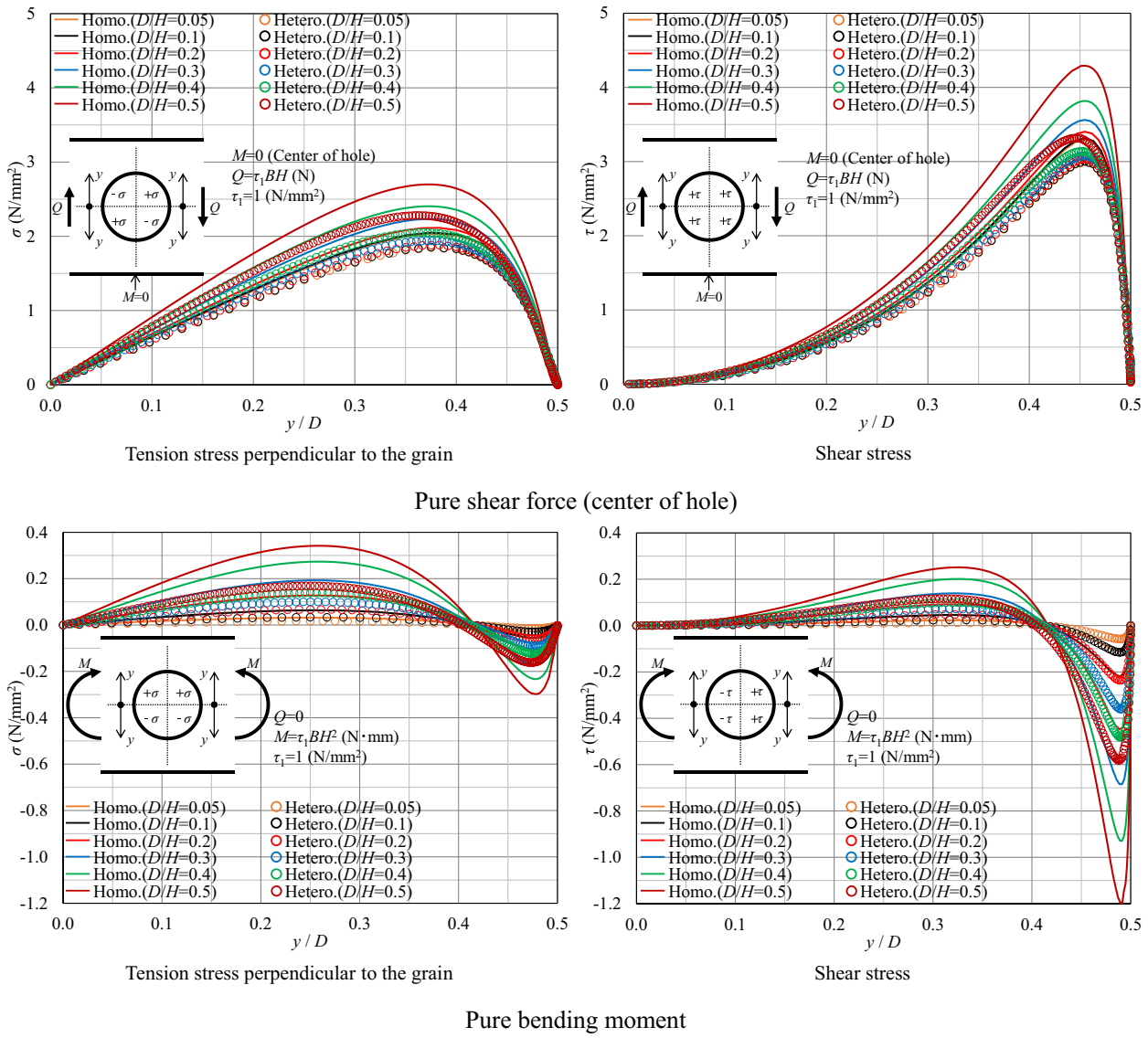

Fig. 24 Stress around the hole, Hetero. E55-F200 and Homo

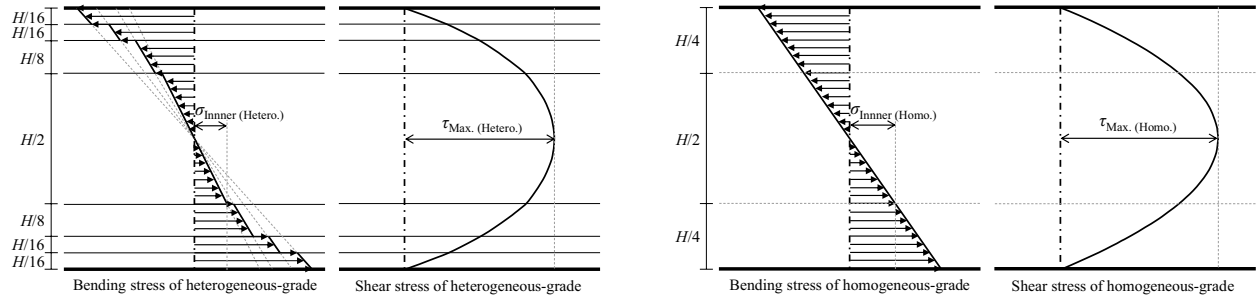

a Bending stress and shear stress in the homogeneous-grade timber and heterogeneous-grade timber

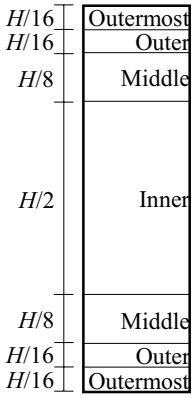

Strength grade of glued laminated timber composed of heterogeneous-grade	Young's modulus (GPa)			
	Outermost	Outer	Middle	Inner
E170-F495	20	18	16	12.5
E150-F435	18	16	14	11
E135-F375	16	14	12.5	10
E120-F330	14	12.5	11	9
E105-F300	12.5	11	10	8
E95-F270	11	10	9	7
E85-F255	10	9	8	6
E75-F240	9	8	7	5
E65-F225	8	7	6	4
E55-F200	7	6	5	3

b Strength grade and lamina placement of glued laminated beams composed of heterogeneous-grade timber

Strength grade of glued laminated timber composed of heterogeneous-grade	k_M	k_Q
	$\frac{\sigma_{\text{Inner}}\ (\text{Hetero.})}{\sigma_{\text{Inner}}\ (\text{Homo.})}$	$\frac{\tau_{\text{Max.}}\ (\text{Hetero.})}{\tau_{\text{Max.}}\ (\text{Homo.})}$
E170-F495	0.72	0.95
E150-F435	0.71	0.95
E135-F375	0.73	0.95
E120-F330	0.74	0.95
E105-F300	0.74	0.95
E95-F270	0.72	0.95
E85-F255	0.69	0.94
E75-F240	0.65	0.94
E65-F225	0.60	0.93
E55-F200	0.53	0.91

c Ratio of stress in the inner lamina

Fig. 25 Bending stress and shear stress in the inner lamina of glued laminated beams composed of heterogeneous-grade timber and glued laminated beams composed of homogeneous-grade timber

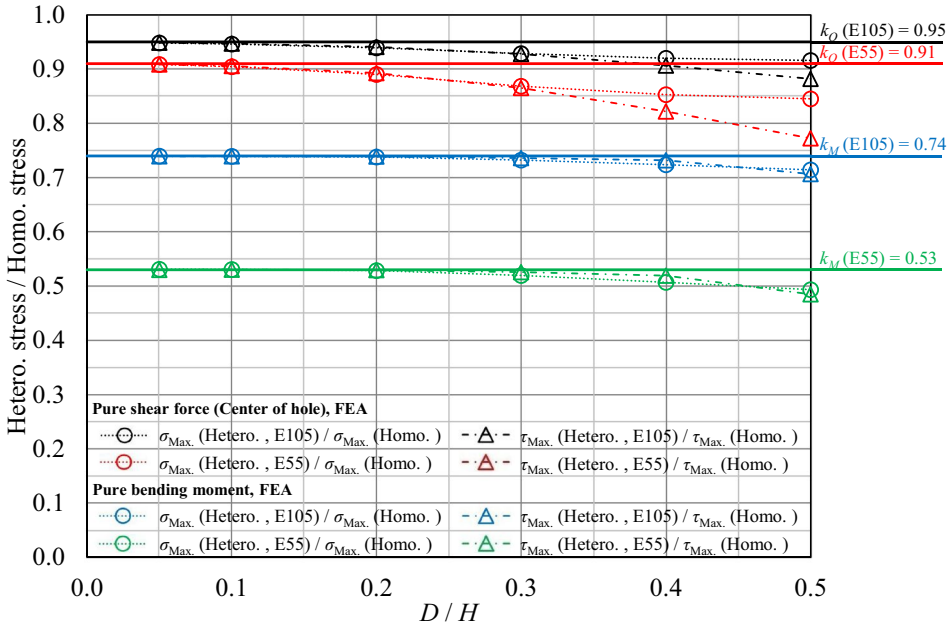

Fig. 26 Ratio of stress in the inner lamina

timber) was 1.05–1.09. The difference in the ratio of material strength to load-bearing capacity of the beams was found to be due to the reduced stresses acting on the holes located in the inner lamina when the glued laminated beams were composed of heterogeneous-grade timber.

3. The tensile stress perpendicular to the grain and shear stresses acting on the holes in the laminated timber with holes of less than half the beam height were lower in the glued laminated beams composed of heterogeneous-grade timber than in the glued laminated beams composed of homogeneous-grade timber. The ratio of the stresses was found to be approximately equal to the ratio of the maximum bending stress or the maximum shear stress acting on the inner layer lamina as determined by Bernoulli–Euler theory. The ratio obtained by the FEA tended to be lower than that obtained by the Bernoulli–Euler theory as the hole size increased. However, using the ratio by Bernoulli–Euler theory to determine the stresses in glued laminated beams composed of heterogeneous-grade timber does not underestimate the stresses and can be applied by the design code.

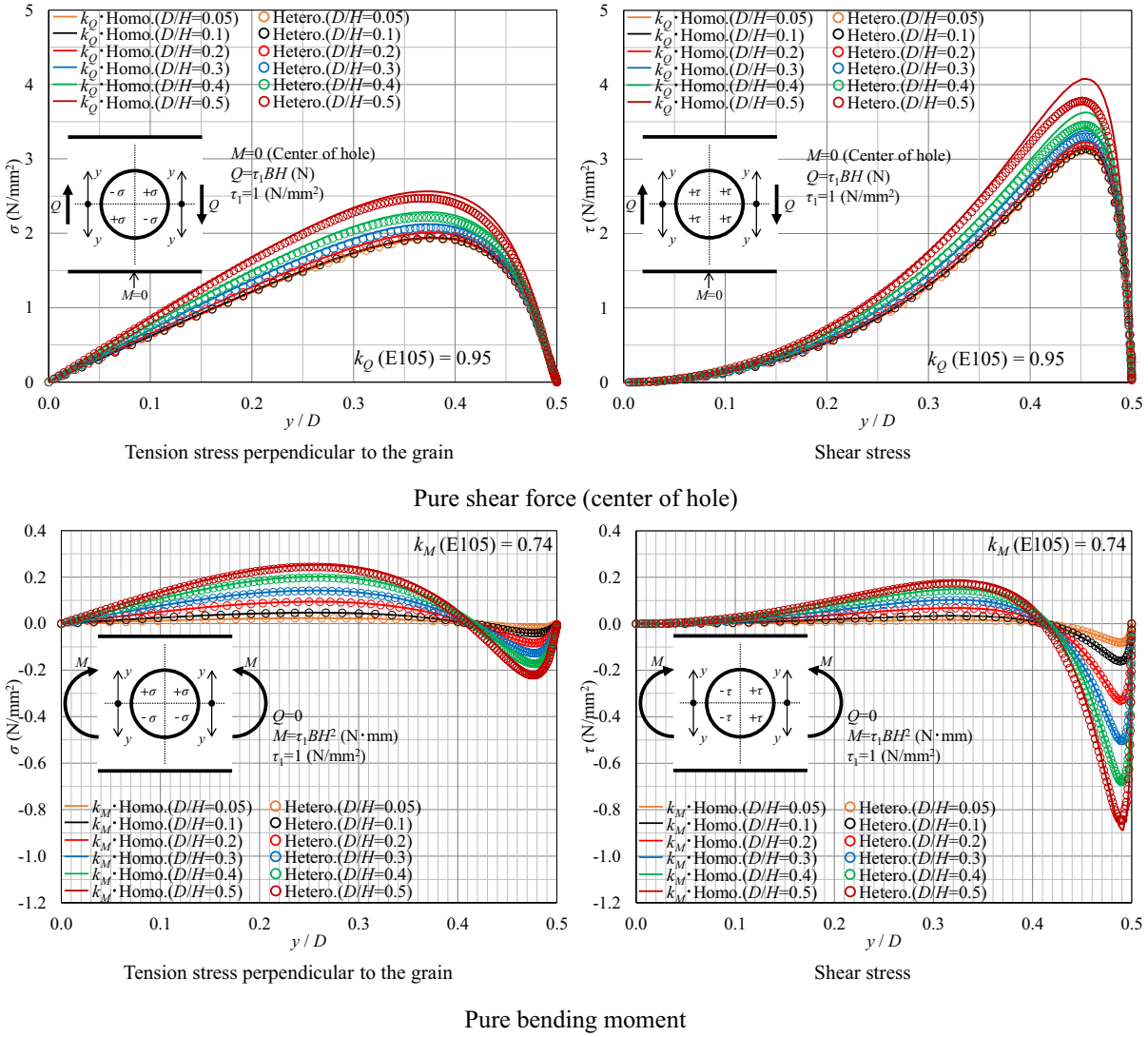

Fig. 27 Stress around the hole, Hetero. E105-F300 and Homo

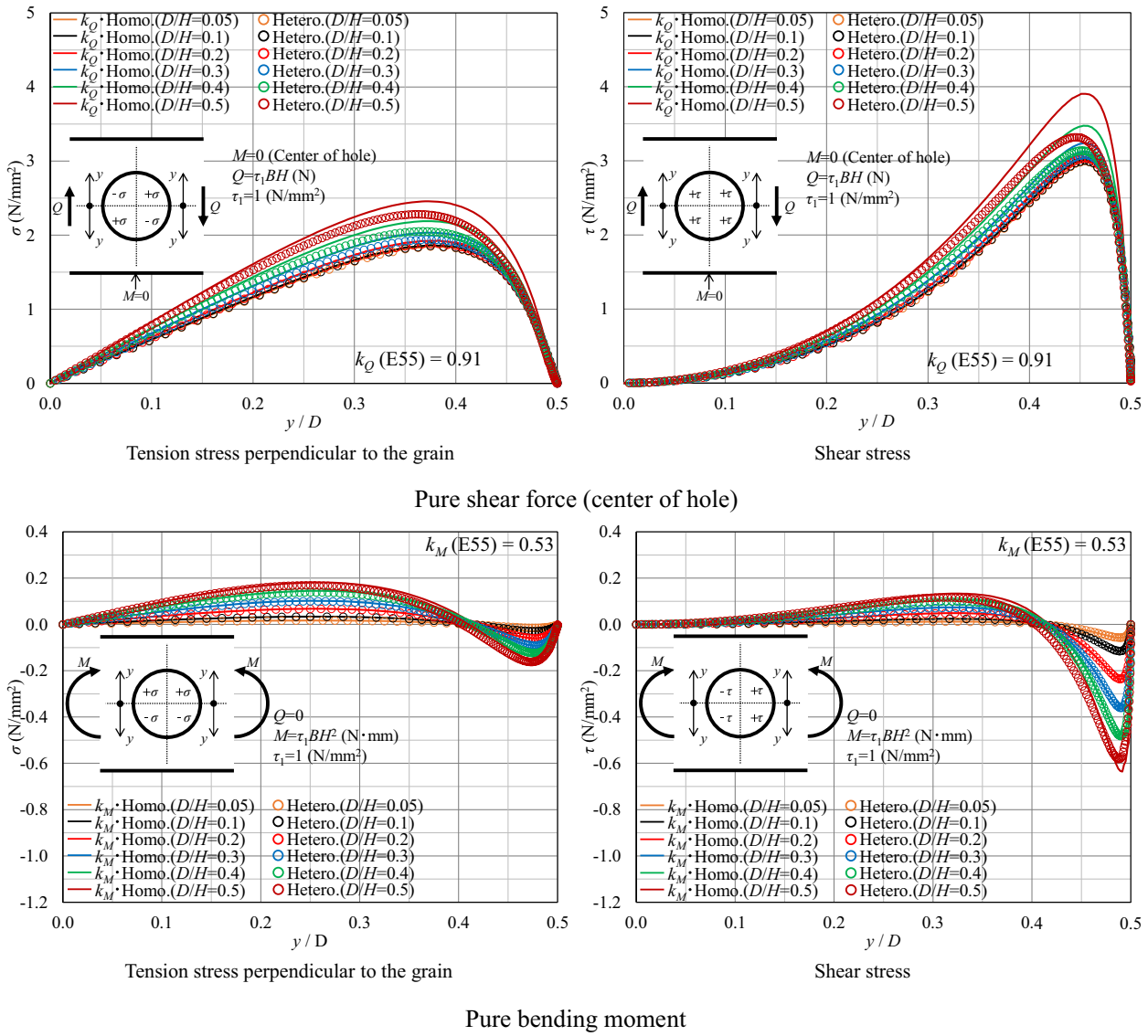

Fig. 28 Stress around the hole, Hetero. E55-F200 and Homo

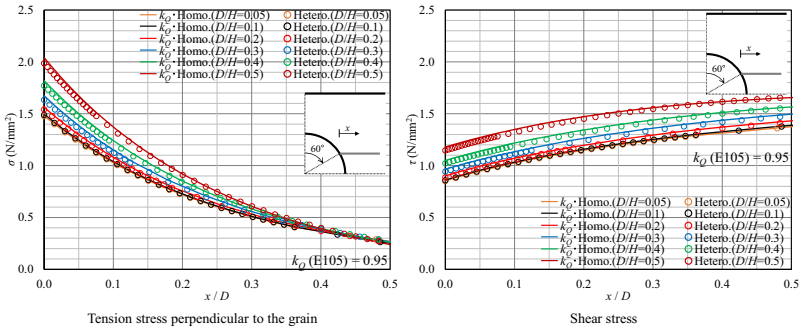

Pure shear force (center of hole), $\theta = 60°$ ($y/D = 0.25$)

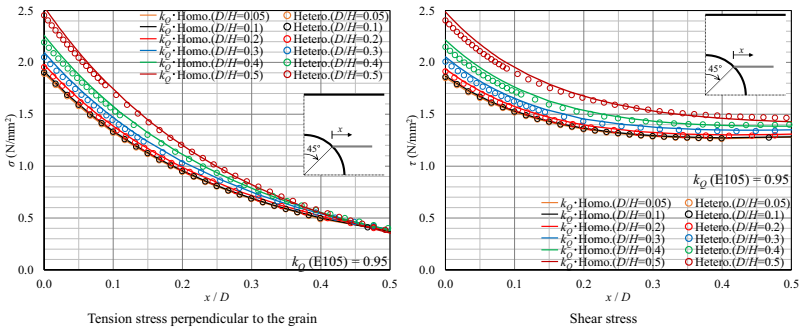

Pure shear force (center of hole), $\theta = 45°$ ($y/D = 0.35$)

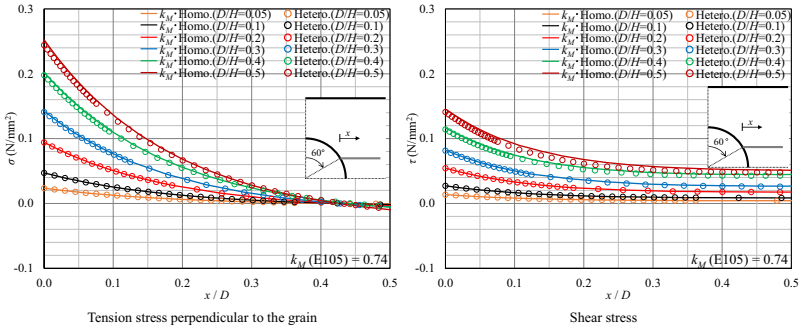

Pure bending moment, $\theta = 60°$ ($y/D = 0.25$)

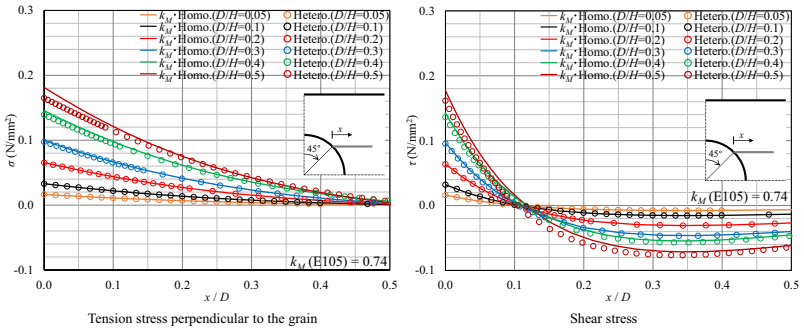

Pure bending moment, $\theta = 45°$ ($y/D = 0.35$)

Fig. 29 Stress distribution in the direction parallel to the grain, Hetero. E105-F300 and Homo

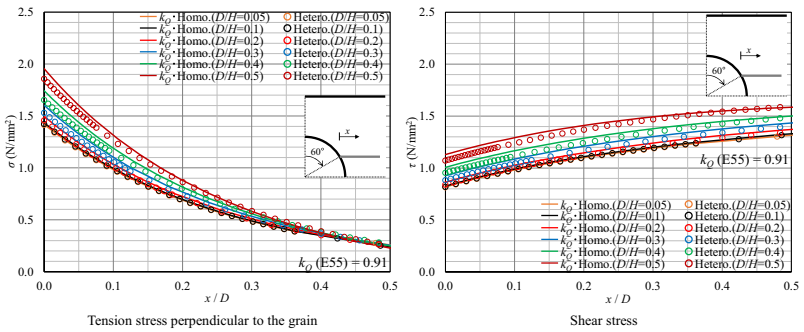

Pure shear force (center of hole), $\theta = 60°$ ($y/D = 0.25$)

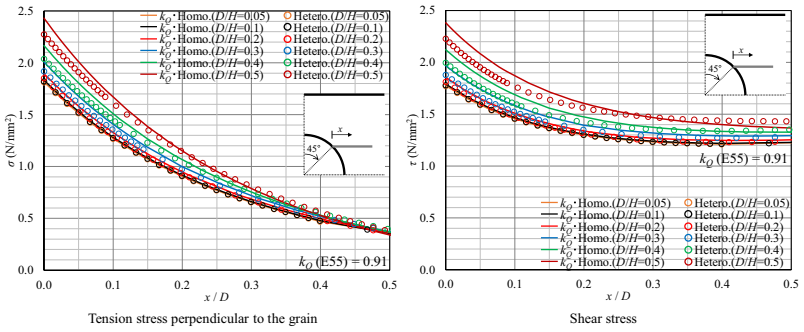

Pure shear force (center of hole), $\theta = 45°$ ($y/D = 0.35$)

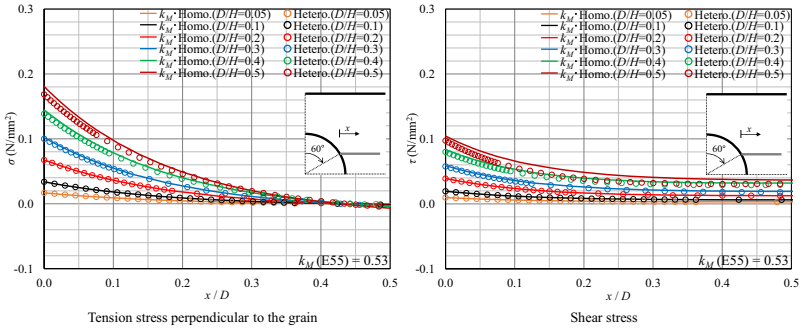

Pure bending moment, $\theta = 60°$ ($y/D = 0.25$)

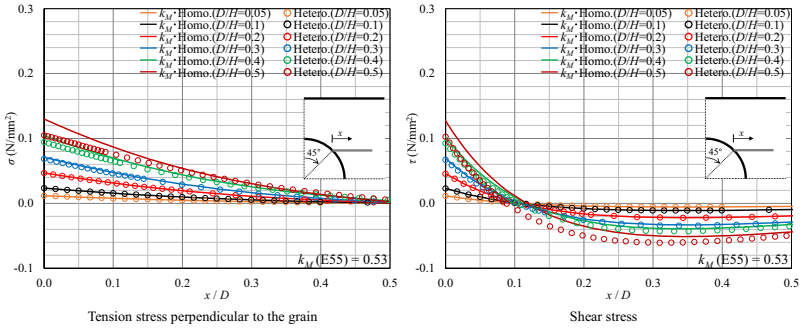

Pure bending moment, $\theta = 45°$ ($y/D = 0.35$)

Fig. 30 Stress distribution in the direction parallel to the grain, Hetero. E55-F200 and Homo

Abbreviations
JAS: Japanese Agricultural Standard; FEA: Finite element analysis; 2D-FEA: Two-dimensional finite element analysis; FE: Finite element.

Acknowledgements
We would like to thank the Hiroshima Prefectural Technology Research Institute Forestry Research Center for conducting the bending tests on the beams and American Journal Experts (https://www.aje.com/) for proofreading this manuscript.

Authors' contributions
SO planned and implemented the research and wrote the manuscript. All authors analyzed the results. All authors read and approved the final manuscript.

Funding
This work was supported by JSPS KAKENHI (Grant numbers 18K13867 and 20K04796).

Availability of data and materials
The test materials, test method, analysis method, and data were recorded as shown in the manuscript. Additional data are available from the corresponding author upon reasonable request.

Competing interests
The authors declare that they have no competing interests regarding the publication of this manuscript.

Author details
[1] Graduate School of Human Life Science, Osaka City University, 3-3-138 Sugimoto, Sumiyoshi-ku, Osaka 558-8585, Japan. [2] National Institute for Land and Infrastructure Management, 1 Tachihara, Tsukuba 305-0802, Japan. [3] Graduate School of Agricultural and Life Sciences, The University of Tokyo, 1-1-1 Yayoi, Bunkyo-ku, Tokyo 113-9657, Japan.

Received: 2 September 2020 Accepted: 6 January 2021
Published online: 19 January 2021

References

1. Hijikata K, Idota H, Yamagishi K (2012) Proposal of design strength for glue-laminated timber beams with a circular through-hole. J Struct Constr Eng (Trans AIJ) 77(673):397–406. https://doi.org/10.3130/aijs.77.397 (**in Japanese**)
2. Aicher S, Höfflin L (2004) New design model for round holes in glulam beams. In: Proceedings of 8th world conference on timber engineering, vol 1, Finland, pp 67–72
3. Noguchi M, Mori T, Miyazawa K (2009) A strength calculation method of the timber with a circular hole. J Struct Constr Eng (Trans AIJ) 74(640):1121–1129. https://doi.org/10.3130/aijs.74.1121 (**in Japanese**)
4. Fröbel J (2016) Limträhandbok Del 2. Svenskt Trä, Stockholm (**in Swedish**)
5. DIN EN 1995-1-1/NA (2010) National Annex—Nationally determined parameters—Eurocode 5: design of timber structures—Part 1–1: general—common rules and rules for buildings. DIN, Berlin (**in Germany**)
6. Aicher S, Höfflin L, Reinhardt HW (2007) Runde Durchbrüche in Biegeträgern aus Brettschichtholz—Teil 2: Tragfähigkeit und Bemessung. Bautechnik 84(12):867–880. https://doi.org/10.1002/bate.200710074 (**in Germany**)
7. Japanese Agricultural Standard (2007) JAS for Glued laminated timber. Japanese Agricultural Standards Association, Tokyo (**in Japanese**)
8. Okamoto S, Araki Y, Akiyama N, Odani R, Aoki K, Inayama M (2020) Study on strength of glued laminated timber beams with round holes: estimation of splitting strength of glued laminated timber composed of heterogeneous grade by finite element analysis. J Struct Constr Eng (Trans AIJ) 85(775):1199–1208. https://doi.org/10.3130/aijs.85.1199 (**in Japanese**)
9. Aicher S, Gustafsson PJ, Haller P, Petersson H (2002) Fracture mechanics models for strength analysis of timber beams with a hole or a notch - a report of RILEM TC-133. Report TVSM-7134, Division of Structural Mechanics, Lund University
10. JIS Z 2101 (2009) Methods of test for woods. Japanese Standards Association, Osaka (**in Japanese**)
11. Gustafsson PJ (1985) Fracture mechanics studies of non-yielding materials like concrete—modeling of tensile fracture and applied strength analyses-. Report No. TVBM-1007, Division of Buildings Materials, Lund Institute of Technology, Lund, Sweden
12. ISO 13910 (2014) Timber structures—strength graded timber—test methods for structural properties. International Organization for Standardization, Geneva
13. NT BUILD 422 (1993) Wood: fracture energy in tension perpendicular to the grain. Nordtest Method, Espoo
14. Forestry and Forest Products Research Institute (2004) Wood industry handbook. Maruzen, Tokyo, p 136, pp 198–199 **(in Japanese)**
15. Kitahara K (1966) Wood physics. Morikitashuppan, Tokyo, p 145, p 164 **(in Japanese)**
16. Larsen HJ, Gustafsson PJ (1990) The fracture energy of wood in tension perpendicular to the grain—results from a joint testing project. In: Proceedings of the CIB-W18A meeting 23, Paper 23-19-2, Lisbon, Portugal, 1990
17. Kanaya N, Yamada T (1964) The relation between the elastic modulus and the porosity of wood. Wood Res 33:47–55 (**in Japanese**)

Publisher's Note